In Situ Gas Phase Diagnostics for Hafnium Oxide Atomic Layer Deposition

J.E. Maslar, W.S. Hurst, D.R. Burgess, W.A. Kimes, N.V. Nguyen, E.F. Moore, J.T. Hodges

National Institute of Standards and Technology, Gaithersburg, MD 20899, USA

Atomic layer deposition (ALD) is an important method for depositing the nanometer-scale, conformal high κ dielectric layers required for many nanoelectronics applications. *In situ* monitoring of ALD processes has the potential to yield insights that will enable efficiencies in film growth, in the development of deposition recipes, and in the design and qualification of reactors. This report will describe the status of a project to develop *in situ* diagnostics for hafnium oxide ALD processes. The focus is on an examination of the utility of Fourier transform infrared spectroscopy and diode laser spectroscopy for optimizing deposition conditions, rather than simply monitoring precursor delivery. Measurements were performed in a single-wafer, warm-wall, horizontal-flow reactor during hafnium oxide ALD involving tetrakis(ethylmethylamino) hafnium and water. Measurements were performed near the wafer surface under a range of deposition conditions in an effort to correlate gas phase measurements with surface processes.

Introduction

Atomic layer deposition (ALD) is increasingly being utilized as a method of depositing the nanometer-scale, conformal layers required for many nanoelectronics applications, including high κ dielectric layers for gate stacks and capacitor structures. However, significant process development issues remain for many of these applications. One potential solution to some process development issues is *in situ* monitoring. *In situ* monitoring of ALD processes has the potential to yield insights that will enable efficiencies in film growth, in the development of deposition recipes, and in the design and qualification of reactors. However, demonstrations of *in situ* monitoring of ALD processes in industrial or simulated industrial ALD reactors are limited.

This report will describe the status of a project to develop *in situ* diagnostics for ALD processes. The current emphasis of this project is on gas-phase optical sensors. Issues being addressed in this work are whether or not gas phase optical diagnostics can be used for more than a precursor delivery monitor, whether such diagnostics can be used to optimize deposition conditions or provide useful validation for practical reactor models, and whether a link can be established between gas phase measurements and film properties that impact device performance. The focus of this report is the examination of Fourier Transform infrared (FTIR) spectroscopy and distributed feedback (DFB) diode laser spectroscopy as diagnostics for ALD. Previous work performed as part of this project has demonstrated that FTIR spectroscopy is sufficiently sensitive to monitor reactant concentrations under realistic ALD conditions.(1) Diode laser-based absorption spectroscopy has also been demonstrated to be sufficiently sensitive to monitor reactant concentrations and even to optimize water purge times under realistic ALD conditions.(2)

However, to these authors' knowledge, these reports are the only such reports involving *in situ* gas phase optical diagnostics of ALD processes that appear in the literature. Hence, while these techniques have shown promise as *in situ* diagnostics for ALD, it is still uncertain how useful these techniques will ultimately be for more than precursor flux monitoring. In this work, measurements were performed near the wafer surface under a range of deposition conditions in an effort to correlate gas phase measurements with surface processes. Measurements were performed in a single-wafer, warm-wall, horizontal-flow reactor during hafnium oxide ALD using tetrakis(ethylmethylamino) hafnium (TEMAH), $Hf[N(C_2H_5)(CH_3)]_4$, and water.

Experimental Method

Materials

Microelectronics-grade TEMAH (Air Products/Schumacher[†]) was purchased in a stainless steel bubbler and employed as received without further purification. For delivery, the TEMAH bubbler was heated to ≈80 ºC to achieve a TEMAH vapor pressure of ≈13.3 Pa (0.1 torr).(3) Deionized water with a resistivity of 18 MΩ · cm or greater at 21 °C was employed. The carrier and purge gas was helium that was obtained as ultra-high-purity grade gas (99.999 % pure) and further purified with a bulk purifier. Deposition was performed on 50 mm diameter (100) silicon wafers. Prior to deposition, wafers were dipped in a 2 % HF solution for 30 s and then exposed to ozone for 4 min.

ALD System

Deposition was performed in a custom designed and built single-wafer, warm-wall, horizontal-flow reactor and pulsed gas injection system. A schematic of the ALD system is shown in Fig. 1. The reactor incorporates optical access near the wafer surface with good gas flow characteristics. Two precursor lines and one extended purge line (with purge gas injection into the chamber through two ports from this line) were employed. Helium was used as the purge/carrier gas for all measurements. For all spectra presented in this work, the nominal flow rate (at standard temperature and pressure) was 75 mL/min (sccm) through each precursor line and 150 mL/min through the purge line for a total nominal flow rate of 300 mL/min in the chamber. Helium gas was always flowing through all three lines, but a precursor was not always entrained in the gas flow. All valves were fast-switching pneumatic diaphragm valves. To inject TEMAH into the reactor, the three-way pneumatic diaphragm valves on this line were opened and the two-way valve was closed for a specified nominal time, T_{TEMAH}. In this state, helium was directed through the TEMAH bubbler. To purge this line, the two three-way valves were closed and the two-way valve was opened. The time interval between the start of this purge and water injection is defined as the TEMAH purge time, P_{TEMAH}. To inject water, the three-way valve on this line was opened and the two-way valve was closed for a specified nominal time, T_{Water}. Water was thereby injected from the water reservoir into the delivery line. The amount of water injected was controlled with a needle valve down-stream of the reservoir and corresponded to approximately 75 mL/min. To purge this line,

---

[†] Certain commercial equipment, instruments, and materials are identified in this publication to adequately specify the experimental procedure. Such identification in no way implies approval, recommendation, or endorsement by the National Institute of Standards and Technology, nor does it imply that the equipment, instruments, or materials identified are necessarily the best available for the purpose.

the three-way valve was closed and the two-way valve was opened. The time interval between the start of this purge and TEMAH injection is defined as the water purge time, P_{Water}. The nominal chamber pressure was ≈133.3 Pa (1 torr) as measured with a capacitance manometer. The reaction chamber was an aluminum tube with a ≈102 mm internal diameter. Optical windows measuring 50 mm in diameter were mounted on opposite sides of the reactor such that the optical path was across the wafer surface. The windows were sealed to the reactor using O-rings that provided a clear aperture measuring ≈41.9 mm in diameter. The distance from the inside surface of the reactor wall to the window inside surface varied from ≈1.5 mm to ≈5 mm. A 50 mm diameter substrate was mounted vertically on a custom-designed chuck such that the gas stream impinged on the substrate surface parallel to the surface normal. The distance from the gas injection port to the wafer surface was ≈253 mm. The chuck consisted of two parts. The base was a stainless steel, sealed chamber containing a 50 mm diameter etched-foil resistance heater patterned to give uniform temperature over its heated area. Isolation of the heater from the deposition chamber insures that no contamination from the heater occurs. An aluminum plate was used to hold a substrate and was mounted on the front of the chuck base chamber. A mineral-insulated metal-sheathed (MIMS) type K thermocouple inserted into a thermocouple well in the face of the base chamber was used for temperature control. Similarly, a MIMS thermocouple mounted into a thermocouple well in the aluminum plate was used for substrate temperature monitoring. The standard measurement uncertainty for these thermocouples is 2.2 °C at 250 °C. To reduce the amount of water adsorbed to the delivery line walls, the lines were heated to ≈110 °C.
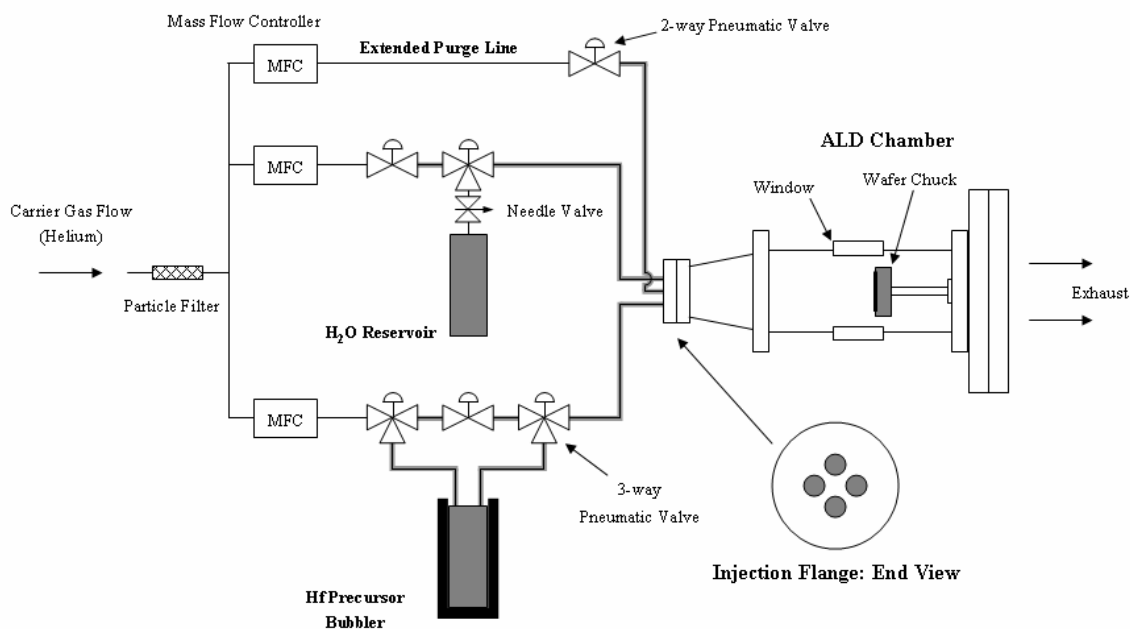

Figure 1. A schematic of the ALD system.

FTIR Spectroscopy

In situ mid-IR absorption measurements were performed using a commercial FTIR spectrometer configured as shown in Fig. 2. The instrument module containing the mid-IR source and interferometer was decoupled from the detector module and three uncoated ellipsoidal aluminum mirrors were used to collect the IR radiation converging out of the interferometer module, transfer the radiation through the ALD reactor chamber, and focus the radiation onto a mercury cadmium telluride detector. A potassium bromide beamsplitter was used for all measurements. The instrument module was purged with dry nitrogen; however, the beam path between the instrument module and the deposition chamber and between the chamber and the detector was not enclosed. The direction of propagation of the IR beam was perpendicular to the wafer surface normal. All spectra taken under ALD conditions were recorded with the beam focus at the center of the reactor and within ≈1 cm of the wafer surface. Uncoated zinc selenide windows were employed on the ALD chamber. All spectra were recorded with $4 \, \text{cm}^{-1}$ spectral resolution.
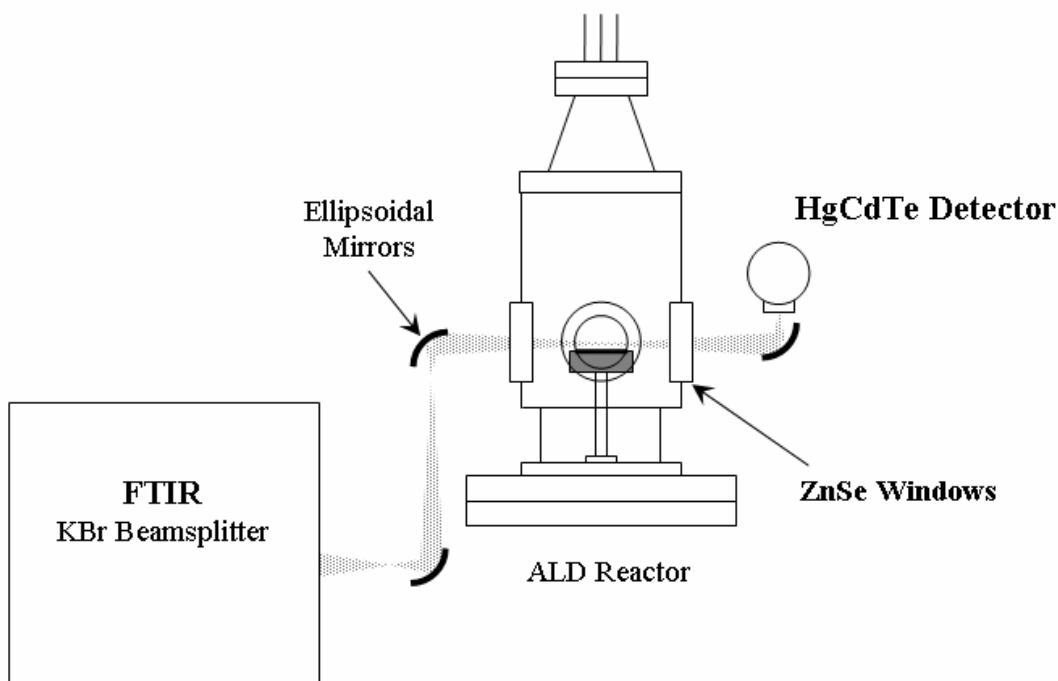

Figure 3. The experimental configuration for *in situ* FTIR spectroscopy.

Reaction precursor and product reference spectra were obtained by recording and co-adding spectra during TEMAH injection and (nominally) complete precursor mixing conditions, respectively. The TEMAH spectra were obtained during injection of 20 cycles of 5 s T_{TEMAH} followed by 5 s P_{TEMAH}. Spectra of (nominally) completely mixed precursors were obtained in a long-residence time chamber, as previously described.(4) These spectra were obtained during injection of 26 cycles with 3 s T_{TEMAH}, 0.1 s P_{TEMAH}, 1 s T_{Water}, and 0.1 s P_{Water}. TEMAH and (excess) water were injected in rapid succession, i.e., short purge times, so as to promote gas phase precursor mixing and complete consumption of TEMAH in the gas phase. Assuming that gas-phase TEMAH and water are present at the same time in the deposition chamber and that TEMAH reacts completely the gas phase reaction can be described by:

$$Hf[N(C_2H_5)(CH_3)]_4 + 2H_2O \rightarrow HfO_2 + 4HN(C_2H_5)(CH_3) \qquad [1]$$
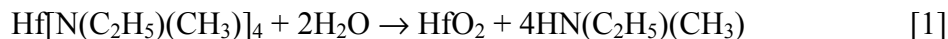
where HfO_2, in this case, is a particulate formed in the gas phase and $HN(C_2H_5)(CH_3)$, subsequently denoted MEA, is a gas phase reaction product. FTIR reference spectra presented in this report were the result of 160 co-added scans each of which were ratioed to a corresponding background spectrum. Background spectra were obtained just prior to a data scan and were recorded with the same spectral conditions and under the same gas injection conditions except with only helium flowing into the chamber. During generation of these reference spectra, no power was supplied to the wafer chuck heater but the TEMAH bubbler, gas delivery lines, and reactor walls were still heated. The monitor thermocouple temperature was 102 °C, with the corresponding wafer surface temperature estimated to be 102 °C ±5 °C.

Spectra recorded during ALD runs were obtained with temporal resolution by employing a variable-time delay trigger for beginning the acquisition of a series of spectra. The effect of varying the FTIR trigger delay time (T_{IR}) is to probe the gas phase species present at different times during a TEMAH or water injection pulse. The first spectrum in each series corresponded to only helium flowing in the chamber and was used as the background spectrum for the whole series. The time-resolved FTIR spectra shown in this report were generated by co-adding the 25 background-ratioed spectra taken at nominally the same time during each of the 25 injection cycles. For all spectra taken during ALD cycles, power was supplied to the wafer chuck heater such that the monitor thermocouple temperature was $\approx$235 °C, with the corresponding wafer surface temperature estimated to be 214 °C ±5 °C (K=1)

DFB Laser Spectroscopy

In situ, time-resolved diode laser-based spectroscopic measurements were performed using a DFB laser operating at a wavelength of 1.392 µm and using a wavelength modulation detection scheme sometimes referred to as second harmonic detection.(5, 6) A schematic of the diode laser-based spectroscopic system is shown in Fig. 4. The temperature and operating current of the laser were both controlled. A function generator was used to impose a 40 kHz sinusoidal modulation on the laser current. The output of the laser was coupled into a fiber which was subsequently split in a 90:10 ratio. The output of each leg was collimated and the higher-power leg of the splitter directed to the ALD chamber and the lower-power leg directed to a reference cell. After passing through the chamber or cell, each beam leg was then focused onto a 10 MHz InGaAs photoreceiver using a fused silica aspheric lens. The reference detector output was supplied to a lock-in amplifier that was set up to detect the 40 kHz modulation (1f). The 1f signal was summed with the 40 kHz sinusoidal modulation to control the laser current so that the laser wavelength remained locked on the water absorption line. The reference cell was charged with $\approx$266.6 Pa (2 torr) of water, had a 20 cm path length, and was configured with fused silica Brewster-angle windows. The signal detector output was supplied to a lock-in amplifier that was set up to detect at 2f. This 2f signal was proportional to the water concentration in the beam path. The ALD chamber was configured with fused silica wedges. All water signal data shown represents the average of 50 injection cycles.
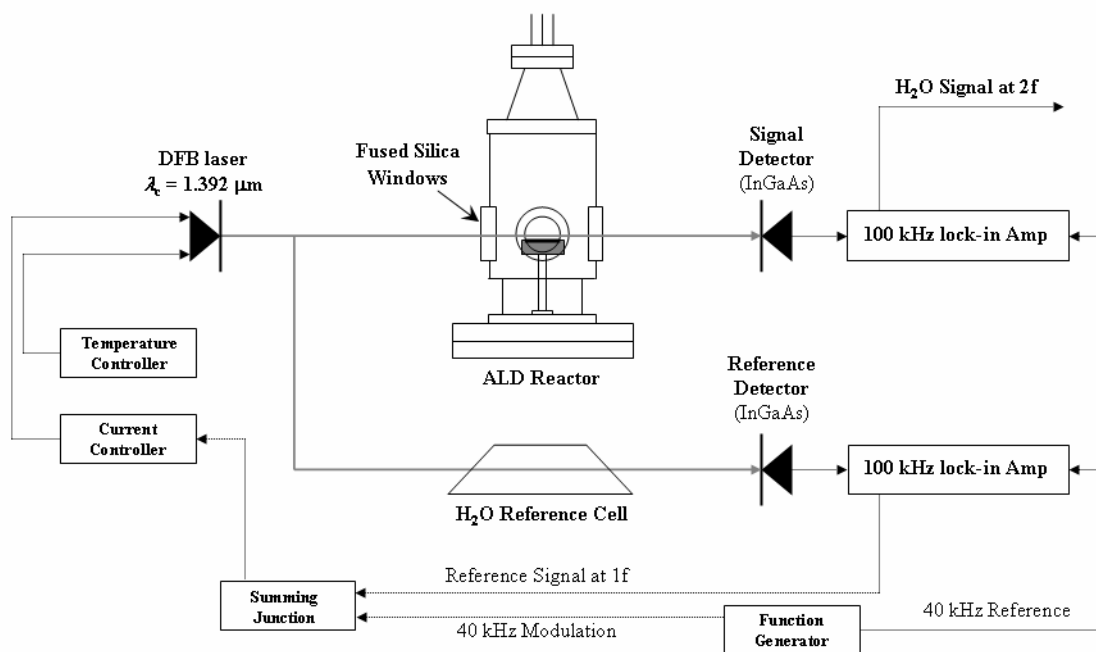
Figure 4. The experimental configuration for DFB diode laser spectroscopy.

Results and Discussion

ALD Chemistry

Assuming complete reaction, the products of the TEMAH and water ALD reaction are hafnium oxide and MEA. For this system, the film deposition reactions can be generally described by the following simplified half reactions (where Hf-OH and Hf-O-Hf[N(C_2H_5)(CH_3)]$_3$ represent the deposition surface on top of the HfO_2 film) (4):

$$\text{Hf-OH} + \text{Hf[N}(C_2H_5)(CH_3)]_4 \rightarrow \text{Hf-O-Hf[N}(C_2H_5)(CH_3)]_3 + \text{HN}(C_2H_5)(CH_3) \qquad [2]$$

$$\text{Hf-N}(C_2H_5)(CH_3) + H_2O \rightarrow \text{Hf-OH} + \text{HN}(C_2H_5)(CH_3) \qquad [3]$$

TEMAH is delivered from a bubbler heated to about 80 °C at which temperature the TEMAH vapor pressure is ≈13.3 Pa (0.1 torr). Water is delivered at room temperature through a needle valve such that flow through the water line into the reactor is approximately 75 mL/min (sccm) of pure water. MEA is a volatile product of the ALD reaction. Hence, the two reactants and only product besides hafnium oxide (assuming complete reaction) potentially can be measured using gas phase diagnostics.

FTIR Spectroscopic Measurements

Reference Spectra. Measured reference spectra were compared to spectra calculated with DFT using B3LYP theory (7, 8) with LANL2DZ basis sets (9) and assuming a temperature of 25 °C. The calculations were performed using commercial software (Gaussian 03, Gaussian, Inc) and the high-performance computational capabilities of the Biowulf Linux cluster at the National Institutes of Health.(10) The final peak wavenumbers in the DFT spectra were obtained by scaling the peak wavenumbers in the

C-H stretching spectral region, ≈ 2800 cm^{-1} to 3150 cm^{-1} (before scaling), by 0.95 and peaks at other wavenumbers by 0.961. Figure 5(a) shows the measured (denoted "Measured") and calculated (denoted "Calculated") TEMAH reference spectra. Figure 5(b) shows the measured and calculated MEA reference spectra. The FTIR instrument lineshape function was not determined, so the DFT spectra are shown with infinitely narrow spectral linewidths. Although a direct comparison of the measured and calculated spectral intensity profiles is difficult, the agreement between the experimental and calculated spectra is good for both TEMAH and MEA. The agreement between the measured spectrum in Fig. 5(b) and the calculated MEA spectrum and the lack of any clear TEMAH-related spectral features in the experimental spectrum in Fig. 5(b) forms the basis of the identification of this spectrum as that of MEA.
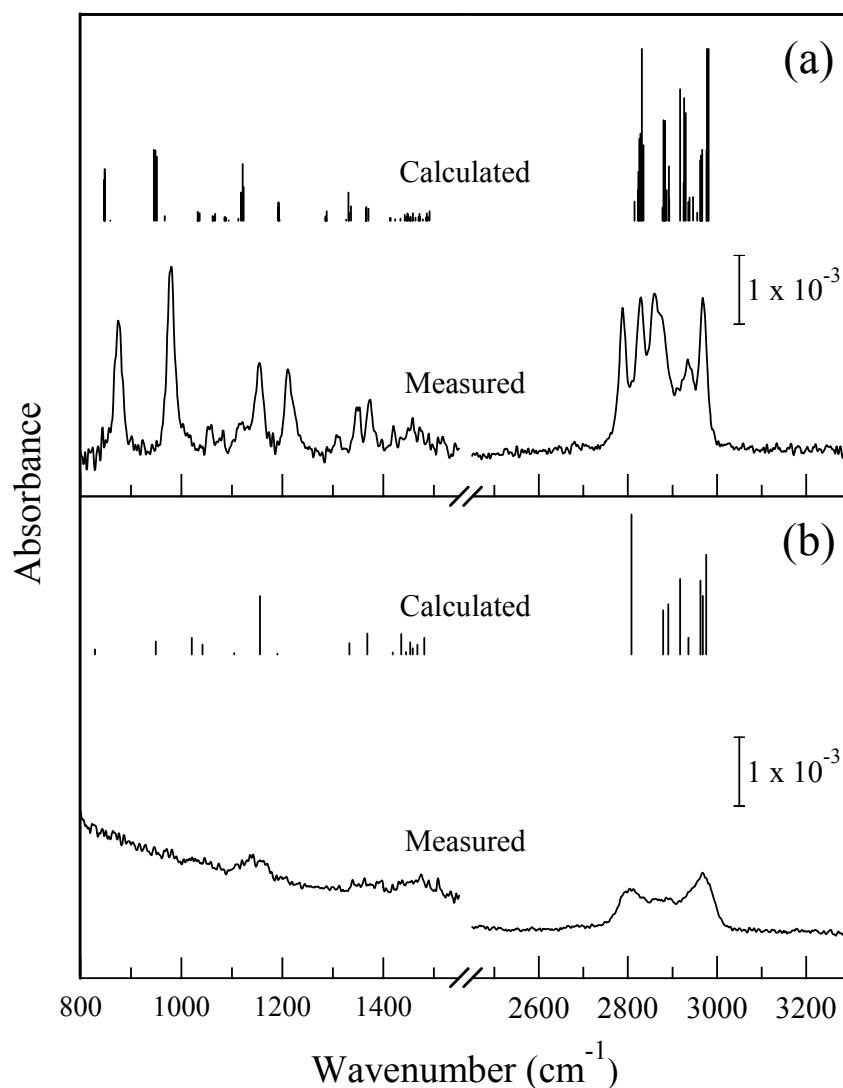

Figure 5. The measured and calculated IR spectra of (a) TEMAH and (b) MEA. The spectra are offset on the absorbance axis for clarity.

While not all IR modes from the DFT calculations can be unambiguously attributed to specific molecular vibrations, a few modes can be identified with a relatively high degree of certainty. From the DFT calculations for TEMAH, the features observed in the

measured TEMAH spectrum at ≈980 cm^{-1} and ≈1154 cm^{-1} are attributed to N-C stretching modes while the feature observed at ≈875 cm^{-1} is attributed to a C-C-N-C backbone mode. From the DFT calculations, the Hf-N stretching modes are expected at ≈560 cm^{-1}. From the DFT calculations for MEA, the feature observed in the measured spectrum at ≈1145 cm^{-1} is attributed to N-C stretching modes. However, it is difficult to deduce the actual lineshape of this feature due to interference from the bending modes of laboratory ambient water that were not removed in the background subtraction process. In both measured spectra, the C-H stretching modes are observed from ≈2750 cm^{-1} to 3000 cm^{-1}.

   In Situ Measurements During ALD. Figure 6 shows the *in situ* time-resolved FTIR spectra recorded near the wafer surface during ALD cycles at different FTIR data collection trigger delay times (T_{IR}). The TEMAH spectrum is shown for comparison, although this spectrum was not measured near the wafer surface. Except for the TEMAH spectrum, the experimental conditions for the spectra shown in Fig. 6 were T_{Water} = 0.1 s, P_{Water} = 15 s, T_{TEMAH} = 3 s, and P_{TEMAH} = 5 s. In Fig. 6, the spectrum taken at T_{IR} = 1.7 s corresponds to the beginning of the TEMAH injection pulse. The T_{IR} = 1.7 s spectrum most closely resembles the MEA spectrum (see Fig. 5(b)). This result indicates that at this point in the injection cycle, surface sites are still reacting with TEMAH to form MEA and that relatively little TEMAH is left unreacted. In the T_{IR} = 1.7 s spectrum, no intense TEMAH signal is observed, even though TEMAH is being injected. This absence is attributed to TEMAH depletion across the thermal/gas velocity boundary layer near the wafer surface. In the type of flow reactor investigated in this work, a thermal/velocity boundary layer exists near the wafer surface.(11) In simple terms, the gas temperature and velocity in this boundary layer can be described as follows. Moving away from the wafer surface, the gas temperature decreases across the boundary layer from the gas temperature at the wafer surface temperature, while the gas velocity increases across the boundary layer from zero velocity at the wafer surface. Although the boundary layer is actually characterized by a decreased gas velocity (relative to the velocity at the gas inlet) and a stagnation flow only exists at the wafer surface, to a first approximation, one can assume that the whole boundary layer is characterized by a stagnation flow to simplify the description of boundary layer processes.(11) Assuming stagnation flow throughout the boundary layer, then reactants only reach the surface via diffusion. In this case and in the presence of a reactive surface, precursors are depleted in the boundary layer. In the absence of a reactive surface, precursors are not depleted in the boundary layer. Therefore, the absence of any TEMAH-related signal during a TEMAH pulse indicates that the surface is still reactive. The T_{IR} = 3.9 s spectrum corresponds to the end of the TEMAH injection pulse and this spectrum most closely resembles the TEMAH spectrum. This result indicates that at this point in the injection cycle TEMAH is not depleted in the boundary layer, i.e., relatively few surface sites are left to react with injected TEMAH. The T_{IR} = 9.6 s spectrum corresponds to the end of the water injection pulse and this spectrum most closely resembles the MEA spectrum. Based on computational fluid dynamics simulations of gas flow in this reactor, the gas residence time near the wafer surface is estimated to be on the order of a few seconds longer than the injection time. Hence, the observation of MEA during water injection indicates that MEA desorbed from the surface at and/or within a few seconds of the measurement time. These results show that FTIR spectroscopy is sensitive to processes occurring in the boundary layer, such as reactant depletion in the presence of reactive surface sites and product desorption from the surface.
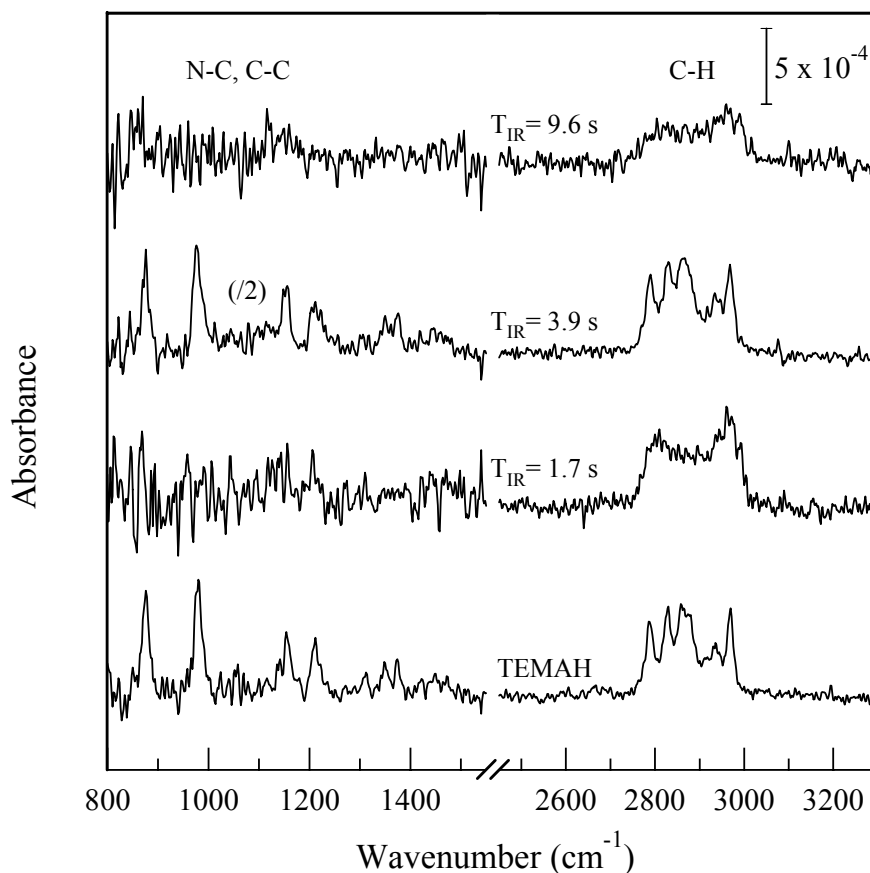
Figure 6. *In situ* FTIR spectra recorded during ALD cycles at different FTIR trigger delay times (T_{IR}). The TEMAH spectrum is shown for comparison. The spectra are offset on the absorbance axis for clarity.

DFB Laser Spectroscopic Measurements

Figure 7 shows the water signal amplitude obtained with the near-IR DFB laser-based absorption measurements in the boundary layer. The two traces correspond to the water signal when only water was injected and when both water and TEMAH were injected. The experimental conditions for water injection were $T_{Water} = 0.1$ s and $P_{Water} = 23$ s, while the conditions for water and TEMAH injection were $T_{Water} = 0.1$ s, $P_{Water} = 15$ s, $T_{TEMAH} = 3$ s, and $P_{TEMAH} = 5$ s. Hence, total exposure times were nominally identical. It is apparent in Fig. 7 that the observed water signal is weaker for TEMAH and water injection versus water injection alone. In addition, the initial water signal is observed later for TEMAH and water injection versus water injection alone. Injection of only water results in a non-reactive surface while injection of water and TEMAH results in a reactive surface (nominally as described by Eqns. [2] and [3]). Therefore, the trends observed in the water and TEMAH trace relative to the water only trace are attributed to water depletion in the boundary layer due to the presence of a reactive surface. Hence, DFB laser spectroscopy is sensitive to reactant depletion in the presence of reactive surface sites.
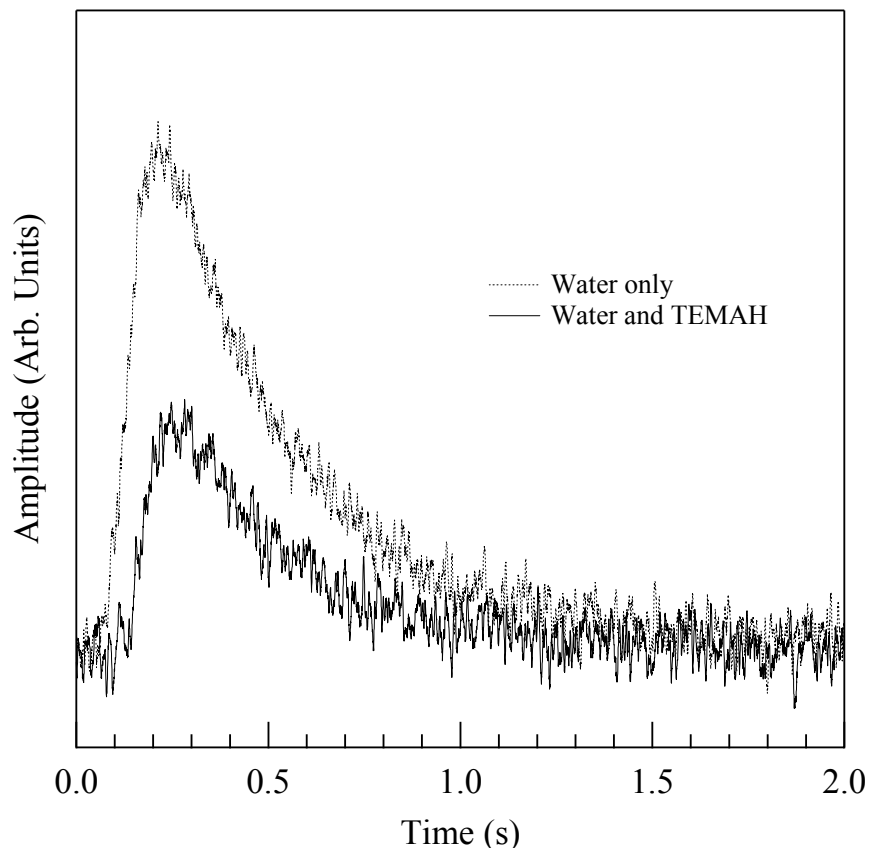
Figure 7. *In situ* water signal recorded with and without TEMAH injection.

Summary and Conclusions

The status of a project to develop *in situ* diagnostics for ALD processes was described. The chemical system under investigation was hafnium oxide ALD using the precursors TEMAH and water. Time-resolved FTIR spectroscopy and DFB diode laser spectroscopy were applied to hafnium oxide ALD in a research-grade, horizontal-flow reactor under a range of deposition conditions. FTIR spectroscopy was shown to exhibit good sensitivity to TEMAH and MEA (the primary reaction product) with moderate time resolution, i.e., adequate sensitivity for precursor delivery monitoring. FTIR spectroscopy was also shown to be sensitive to TEMAH depletion across and MEA desorption into the near-surface boundary layer in the presence of a reactive surface. DFB diode laser spectroscopy was shown to exhibit excellent sensitivity to water with high time resolution and to be sensitive to water depletion across the boundary layer. These results demonstrate that gas-phase measurements in the boundary layer can be linked to ALD surface processes.

Acknowledgments

References

1. J. E. Maslar, W. S. Hurst, D. R. Burgess, Jr., W. A. Kimes, N. V. Nguyen and E. F. Moore, in *Frontiers of Characterization and Metrology for Nanoelectronics*, D. G. Seiler, A. C. Diebold, R. McDonald, C. M. Garner, D. Herr, R. P. Khosla and E. M. Secula Editors, p. 121, American Institute of Physics, Melville, NY (2007).
2. R. Inman, A. Deshpande, D. Chraibi and G. Jursich, in *SEMI Technology Symposium: Innovations in Semiconductor Manufacturing*, p. 205, San Jose, CA (2003).
3. D. M. Hausmann, E. Kim, J. Becker and R. G. Gordon, *Chem. Mater.*, **14**, 4350 (2002).
4. J. E. Maslar, W. S. Hurst, D. R. Burgess, W. A. Kimes and N. V. Nguyen, *ECS Transactions*, **2**, 133 (2007).
5. J. Reid and D. Labrie, *Appl. Phys. B*, **26**, 203 (1981).
6. W. H. Weber, J. T. Remillard, R. E. Chase, J. F. Richert, F. Capasso, C. Gmachl, A. L. Hutchinson, D. L. Sivco, J. N. Baillargeon and A. Y. Cho, *Appl. Spectrosc.*, **56**, 706 (2002).
7. A. D. Becke, *J. Chem. Phys.*, **98**, 5648 (1993).
8. C. T. Lee, W. T. Yang and R. G. Parr, *Phys. Rev. B*, **37**, 785 (1988).
9. P. J. Hay and W. R. Wadt, *J. Chem. Phys.*, **82**, 270 (1985).
10. Biowulf Linux Cluster. http://biowulf.nih.gov (accessed 2006).
11. G. B. Stringfellow, in *Organometallic Vapor-Phase Epitaxy : Theory and Practice, 2nd Ed.*, p. 297, Academic Press, San Diego (1999).